

EUROPEAN ORGANIZATION FOR NUCLEAR RESEARCH

CERN-PPE/90-151

October 15, 1990

# Constraints on the Standard Model from Experimental Studies of the Z Pole

Enrique Fernández\*

CERN/PPE Div

and

Universitat Autònoma de Barcelona  
Laboratori de Física d'Altes Energies  
Bellaterra, Barcelona, Spain

## Abstract

The measurements of the mass and widths of the Z resonance obtained by the LEP experiments are presented and their averages calculated. The interpretation of these quantities in the framework of the Standard Model, and the constraints on its parameters resulting from their values, are discussed. The results of the LEP averages are:  $M_Z = 91.177 \pm 0.031 \text{ GeV}/c^2$ ,  $\Gamma_Z = 2497 \pm 15 \text{ MeV}$ ,  $\Gamma_{lepton} = 83.9 \pm 0.7 \text{ MeV}$ ,  $\Gamma_{hadron} = 1764 \pm 16 \text{ MeV}$ ,  $\Gamma_{invisible} = 482 \pm 16 \text{ MeV}$ ,  $\Gamma_{hadron}/\Gamma_{lepton} = 21.08 \pm 0.20$ ,  $\sigma_h^0 = 41.78 \pm 0.53 \text{ nb}$ ,  $\Gamma_e = 83.6 \pm 0.9 \text{ MeV}$ ,  $\Gamma_\mu = 83.8 \pm 1.2 \text{ MeV}$ ,  $\Gamma_\tau = 83.3 \pm 1.4 \text{ MeV}$ ,  $N_\nu = 2.89 \pm 0.10$ ,  $\sin^2(M_Z^2) = 0.2300 \pm 0.0020$ ,  $\alpha_s(M_Z^2) = 0.16 \pm 0.03$ .

\*Talk given at the Neutrino-90 Conference, CERN, June 1990. (The LEP results have been updated with those presented at the 25th International Conference on High Energy Physics in Singapore, August 1990).

# 1 Introduction

One of the main goals of the SLC and LEP experiments during the first year of data analysis has been the measurement of the energy dependence of the  $e^+e^-$  annihilation cross-section into pairs of fermions near the Z pole, the so-called Z line shape. As it has been extensively discussed [1], [2] the detailed measurement of the line shape allows a number of fundamental tests of the Standard Model.

First, the Z mass,  $M_Z$ , can be obtained with great precision. This quantity is usually taken, when discussing electroweak physics at  $M_Z$  energies, as one of the three fundamental parameters of the gauge sector of the model, together with  $\alpha$  and  $G_\mu$ . The precision with which  $M_Z$  can be measured sets the scale for any other precise test of the electroweak theory. Second, both the shape and magnitude of the cross-section are sensitive, through radiative corrections, to yet unknown parameters of the model, such as the masses of the top quark and of the Higgs boson. The radiative corrections have been studied in detail [3] and the value of these parameters can be constrained from the data. Third, the line shape is also sensitive to the existence of new particles not contemplated in the Standard Model, and to deviations of this model beyond its minimal structure [4].

When analyzing the LEP and SLC data all experiments have followed the philosophy suggested in [2],[5] which is also adopted here to present the data. Namely, the line shape, or rather the line shapes into hadrons and leptons, are fitted to a model independent parametrization of the cross-section in terms of the mass and the total and partial widths of the Z. Once the widths are obtained, their interpretation within the Standard Model allows the calculation of more commonly used parameters, such as  $\sin^2 \theta_W$ , or when combined with measurements of asymmetries, the vector and axial vector couplings of the Z to fermions. The model independent quantities can also be interpreted, within the Standard Model, to constraint the unknown parameters, namely the top and Higgs masses.

This talk is organized as follows: section 2 covers very briefly the methods used to measure the cross-sections. In section 3 the main formulae describing the line shape are summarized. In section 4, the fits needed to extract the mass

and widths of the Z from the data are described and the results are summarized. The average of the LEP experiments, taking into account the systematic errors common to all of them, are presented in section 5, together with the comparison of the results with the SM predictions. SLC data are also shown in some of the plots but are not used in the averages due to their much larger statistical errors. The constraints on Standard Model parameters resulting from these data, in particular on the number of neutrino families,  $\sin^2 \theta_W(M_Z^2)$ ,  $\alpha_s$  and the mass of the top, are described in section 6.

Other results from LEP data presented in this Conference are covered in [6], [7], [8] and the status of the Standard Model is covered in [9].

## 2 The hadronic and leptonic line shapes

All four LEP experiments, ALEPH, DELPHI, L3 and OPAL, have published measurements of the total cross-section as a function of the total center of mass energy of  $e^+e^-$  annihilation into hadrons (the hadronic line shape) and into pairs of leptons (leptonic line shapes) [10], [11], [12], [13]. The Mark II experiment at the SLC has also published the  $e^+e^-$  annihilation cross-section into hadrons, muons and taus [14]. The data presented here are the latest available from the experiments as of the time of this writing (August 1990) and almost all of them were presented at the the 25th International Conference on High Energy Physics at Singapore [15],[16],[17],[18], [19]. Mark II results are from [14].

The measurement of the line shapes is in principle simple. It requires: i) to count the number of  $e^+e^-$  annihilation events into hadrons or into leptons in a given detector acceptance for each center of mass energy, ii) to correct this number for possible inefficiencies and backgrounds, iii) to extrapolate the number of events to full  $4\pi$  acceptance (with suitable Monte Carlo), iv) to measure the luminosity, which in  $e^+e^-$  machines is usually achieved by counting the number of Bhabha events at small angles, where the Bhabha cross-section can be calculated with negligible dependence on unknown parameters.

The selection of hadronic events is based on the number of charged tracks and their momenta as observed by tracking detectors (as it is the case in one of the

selection methods of ALEPH and DELPHI), or on the number of calorimetric clusters and their energy (as it is done by L3 and OPAL), or in a combination of both (ALEPH and DELPHI). Typically more than one selection method is used by each experiment and the reader is referred to references [10] to [13] for detailed descriptions of these methods. The selection of leptonic events relies on the low multiplicity of these events and on the characteristics of their visible momentum and energy deposition in the calorimeters. Fig.1 shows the four types of events as seen in the ALEPH detector.

LEP has taken data at several energy points located symmetrically with respect to that of maximum cross-section. The total luminosity delivered by the machine until the end of August 1990 is of the order of  $10 \text{ pb}^{-1}$ . However, the data samples available to any single experiments for analysis will be somewhat smaller, since the efficiency of data collection is not 100%. The analysis of these data has not yet been completed. Table 1 is a summary of the data samples used by the four experiments to extract the hadronic lineshapes described in this paper. The number of events is only approximate, since, as already mentioned, more than one selection method is typically available. In Table 1 the errors on the luminosity measurements, which affect the normalization into cross-sections, are also shown.

Table 2 summarizes the data samples and systematic errors of the leptonic cross-sections, not including the luminosity error.

Figures 2-7 show the hadronic and leptonic lineshapes measured by the four LEP experiments. The curves are the fits described in section 4.

### 3 Model independent description of the Line Shapes

The tree-level cross-section for  $e^+e^- \rightarrow f\bar{f}$ , assuming that only the Z and the  $\gamma$  mediate the reaction, can be written as

$$\sigma(s) = \frac{s}{(s - M_Z^2)^2 + (M_Z\Gamma_Z)^2} \left[ \frac{12\pi\Gamma_e\Gamma_f}{M_Z^2} + \frac{I(s - M_Z^2)}{s} \right] + \frac{4\pi\alpha^2}{3s} Q_f^2 N_c^f \quad (1)$$

where the last term comes from the exchange of the photon, the first from the exchange of the resonant  $Z$ , parametrized in the form of a spin-1 Breit-Wigner, and the second is the interference. In this formula,  $\alpha$  is the QED coupling constant, and  $Q_f$  and  $N_c^f$  are the electric charge and color number of fermion  $f$  respectively. The total width  $\Gamma_Z$  is given by

$$\Gamma_Z = \sum \Gamma(Z \rightarrow f\bar{f}) \quad (2)$$

where the sum extends to all the fermions to which the  $Z$  can couple. Assuming that only vector and axial vector couplings are present, the partial width  $\Gamma_f \equiv \Gamma(Z \rightarrow f\bar{f})$  and the interference term  $I$  can be calculated as

$$\Gamma_f = \frac{\alpha M_Z N_c^f}{3} F \sqrt{1 - \frac{4m_f^2}{M_Z^2}} \left[ g_{Vf}^2 \left( 1 + 2\frac{m_f^2}{M_Z^2} \right) + g_{Af}^2 \left( 1 - 4\frac{m_f^2}{M_Z^2} \right) \right] \quad (3)$$

$$I = -\frac{8\pi\alpha^2 Q_f N_c^f}{3} F (g_{Vf} \cdot g_{Ve}) \quad (4)$$

$$F = \frac{G_F M_Z^2}{2\sqrt{2}\pi\alpha} \quad (5)$$

where  $G_F$  is the Fermi constant,  $m_f$  is the mass of fermion  $f$ , and  $g_{Vf}$ ,  $g_{Af}$  are the vector and axial vector neutral current coupling constants for fermion  $f$ .

Radiative corrections strongly modify these formulae. These corrections have been studied in detail over the past few years [3], and it is thanks to this vast amount of work that the line shape can be adequately described in a relatively simple way.

Ignoring for the moment the case of Bhabha scattering, the cross-section for the inclusive reaction  $e^+e^- \rightarrow f\bar{f}X$ , where  $X$  includes photons or gluons, can be written as [2],[20]

$$\sigma(s) = \int_0^{X_{\max}} H(x, s) \hat{\sigma}(s(1-x)) dx \quad (6)$$

where  $H(x,s)$  is the probability of radiating a fraction  $x$  of the total center of mass energy,  $s$ , from the incoming initial state  $e^+e^-$ , and  $\hat{\sigma}(s(1-x))$  is the cross-section at the reduced center of mass energy. This convolution effectively takes into account the largest part of the QED or photonic corrections (those involving real or virtual photon lines only), namely initial state radiation. Suitable radiator functions have been calculated to order  $\alpha^2$  and with soft photon exponentiation [21]. The effect of the radiator function is to displace the position of the peak of the cross-section by about +110 MeV with respect to the tree-level formula and to reduce the peak cross-section by about 25%.

Purely weak corrections as well as final state photon and gluon radiation, can be effectively included in the reduced cross-section  $\hat{\sigma}$ . A model-independent expression for  $\hat{\sigma}$  has been suggested in [2], [5]

$$\hat{\sigma}(s) = \frac{s}{(s - M_Z^2)^2 + \left(s \frac{\Gamma_Z}{M_Z}\right)^2} \left[ \frac{12\pi\Gamma_e\Gamma_f}{M_Z^2} + \frac{\bar{I}(s - M_Z^2)}{s} \right] + \frac{4\pi\bar{\alpha}^2}{3s} Q_f^2 N_C^f \quad (7)$$

This is similar in form to the Born-level formula but there are some important differences. The Breit-Wigner has an  $s$ -dependent width (which arises when including vacuum polarization corrections). This has the effect of displacing the peak position by about -35 MeV. The total and partial widths are now the physical widths, including most of final state radiation and weak corrections, and therefore cannot be written in principle as in formula (3) (see section 2). The interference term and the QED coupling constant are also affected by radiative corrections and hence the symbols  $\bar{\alpha}$  and  $\bar{I}$ . The model-independent formula is only approximately valid, since it cannot incorporate some non-factorizable corrections, such as initial-final state radiation interference and box diagrams. It is nevertheless adequate for the description of the data with the present statistical and systematic errors. Quantitative analysis of its validity have been done in [22], [20].

This formula can be used to fit the line shape into a given  $f\bar{f}$  final state and extract the widths. In the formula the radiative corrections to  $\alpha$  are very well known (since they are dominated by light particles, see section 6) and the interference term is small (less than 0.4 per mil at tree-level in the Standard Model). In practice the interference  $\bar{I}$  can be calculated in the Standard Model with a negligible error introduced in the extraction of the widths. The formula of the line shape depends then on 3 parameters:  $M_Z$ ,  $\Gamma_Z$  and the product of the partial widths  $\Gamma_e\Gamma_f$ .

The three parameters  $M_Z$ ,  $\Gamma_Z$  and  $\Gamma_e\Gamma_f$  can be extracted from a fit to the data. The mass and the total width are best determined from the hadronic line shape (due to the smaller statistical and systematic errors). The electronic width  $\Gamma_e$  can be obtained from fitting the line shape into electrons but the extraction of  $\Gamma_h$ ,  $\Gamma_\mu$  or  $\Gamma_\tau$  requires to combine the line shape (or at least the branching ratio) into these final states with the  $e^+e^-$  final state. A simultaneous fit to all the line shapes, with the full correlation error matrix, is perhaps the most convenient way of extracting the parameters.

The formulae above refer to  $s$ -channel cross-sections. In the case of Bhabha scattering,  $t$ -channel diagrams also contribute to the cross-section, especially in the forward direction where they become dominant. The procedure currently adopted by all the experiments is to subtract from the measured Bhabha cross-section the contribution of the  $t$  channel and  $s$ - $t$  interference terms and treat the resulting lineshape as induced by  $s$ -channel diagrams. The problem here is that no complete order  $\alpha^2$  calculation of the Bhabha cross-section exists yet. In the case of ALEPH the  $t$  and  $s$ - $t$  interference terms were evaluated with the formula of reference [23]. In the reduced phase space on which the formula and data were utilized, it is estimated that the error on the  $t$ -channel contribution

to the Bhabha cross-section is 0.5% [15]. L3 uses a more recent version of this formula [24] as well as a more recent calculation [25]. DELPHI and OPAL have used this recent calculation [25] which has an estimated uncertainty of 0.5% without the requirement of acceptance cuts.

## 4 The fits to the line shapes

As it has been remarked above, the expression for the lineshape into a given final state  $f\bar{f}$  depends on 3 parameters:  $M_Z$ ,  $\Gamma_Z$  and the product of the partial widths  $\Gamma_e\Gamma_f$ . A fit to any lineshape can provide these 3 parameters (or any set of three parameters related to them). From the simultaneous fit to several lineshapes it is possible to obtain the partial widths into hadrons and each lepton species individually.

Experimentally it is convenient to define the partial width into hadrons,  $\Gamma_{had}$ , the leptonic width,  $\Gamma_l$ , and the invisible width,  $\Gamma_{inv}$ , by

$$\Gamma_{had} = \sum_{\text{quarks}} \Gamma(Z \rightarrow q\bar{q}) \quad (8)$$

$$\Gamma_l = \frac{1}{3} \sum_{e,\mu,\tau} \Gamma(Z \rightarrow \ell^+\ell^-) \quad (9)$$

$$\Gamma_{inv} = \Gamma_Z - \Gamma_{had} - 3 \cdot \Gamma_{lept} \quad (10)$$

The hadronic peak cross-section,  $\sigma_{had}^0$ , is related to the ratio of the widths

$$\sigma_{had}^0 = \frac{12\pi}{M_Z^2} \frac{\Gamma_e\Gamma_{had}}{\Gamma_Z^2} \quad (11)$$

The values reported by the LEP experiments are summarized in Table 3. The statistical and systematic errors, if reported separately, have been added in quadrature to make this table.

The different experiments use different fitting formulae and make several fits with different assumptions such as imposing or not Standard Model constraints in the fits. The numbers in Table 3 are “model-independent” numbers, obtained with essentially the same assumptions by the different experiments. A brief summary of the procedures used to obtain them is the following:

In ALEPH [15] the hadronic and inclusive leptons lineshapes are fitted simultaneously, with a slightly modified version [22] of the formula given in [2], and with the initial state radiation formulae of [21] to obtain 4 parameters,  $M_Z$ ,  $\sigma_{had}^0$ ,  $\Gamma_Z$  and  $R = \Gamma_{had}/\Gamma_l$ , or, alternatively,  $M_Z$ ,  $\Gamma_Z$ ,  $\Gamma_h$ ,  $\Gamma_l$ . The numbers on Table 3 for these quantities, as well as for  $\Gamma_{inv}$ , come from such a fit. The hadronic and the three leptonic,  $e^+e^-$ ,  $\mu^+\mu^-$  and  $\tau^+\tau^-$ , lineshapes are also fitted simultaneously to obtain the 6 parameters  $M_Z$ ,  $\Gamma_Z$ ,  $\sigma_{had}^0$ ,  $\Gamma_{had}/\Gamma_e$ ,  $\Gamma_{had}/\Gamma_\mu$ ,  $\Gamma_{had}/\Gamma_\tau$ . The

3 leptonic widths in Table 3 are obtained from these numbers. The results of the fits are shown by the curves in Figs. 2 and 3.

In DELPHI [16] the hadronic and leptonic lineshapes are fitted simultaneously (assuming universality) with the formulae of [26] to obtain 4 parameters:  $M_Z$ ,  $\Gamma_Z$ ,  $\Gamma_{had}$  and  $R$ . From these  $\Gamma_l$  and  $\Gamma_{inv}$  are calculated. Fixing the values of  $M_Z$  and  $\Gamma_Z$  to those obtained above, a fit to the three leptonic lineshapes gives  $\Gamma_e$ ,  $\Gamma_\mu$  and  $\Gamma_\tau$ . The value of  $\sigma_{had}^0$  in the table comes from a 3 parameter fit to the hadronic lineshape alone. The curves in Fig. 4 show the results of the fits.

In L3 [17] the hadronic and muonic data are fitted with several formulae [27], [5], [28] to obtain the values of  $M_Z$ ,  $\Gamma_Z$ ,  $\Gamma_{had}$ ,  $R$  and  $\Gamma_{inv}$  quoted in Table 3. The leptonic widths  $\Gamma_e$ ,  $\Gamma_\mu$ ,  $\Gamma_\tau$  and  $\Gamma_l$  come from updated samples from those published previously [17]. The curves in Fig. 5 and 6 show the results of the fits.

In OPAL [18] the energy dependence of the hadronic cross-section and the energy dependence and forward-backward asymmetry of the leptonic cross-sections are fitted simultaneously using the formulae described in [18], [29] and [25]. From the combined fit, 5 parameters are obtained:  $M_Z$ ,  $\Gamma_Z$ ,  $\Gamma_{had}$ ,  $\Gamma_l$  and  $\hat{a}^2\hat{v}^2$  (the effective axial vector and vector couplings at  $\sqrt{s} = M_Z$ , see section 6). The numbers for  $M_Z$ ,  $\Gamma_Z$ ,  $\Gamma_{had}$ ,  $\Gamma_l$  (and  $\Gamma_{inv}$  which is derived from them) are directly comparable to ALEPH's and DELPHI's 4-parameter fit. Fits without the assumption of lepton universality are also performed by OPAL to obtain the individual leptonic partial widths  $\Gamma_e$ ,  $\Gamma_\mu$ ,  $\Gamma_\tau$ . The curves in Fig. 7 show the results of the fits.

## 5 The average of the LEP experiments and the comparison with the Standard Model predictions

The last column in Table 3 gives the averages of the four LEP experiments. The central values are the weighted (by the inverse of the square of the error) averages of the reported values. However, when calculating the error on the average, care must be taken of the fact that there are systematic errors common to all experiments [19], [30], of which the most important, aside from the overall uncertainty in the LEP energy scale, is that due to the theoretical error on the evaluation of the Bhabha cross-section at low angles, needed for the calculation of the luminosities. However, the common sources of errors affect differently the different experiments and there is no simple way of estimating what their exact effect on the averages is. A brief explanation of what has been done here is the following:

The error in the mass is dominated by the uncertainty in the LEP energy scale, a common systematic error for all LEP experiments, which is added in



quadrature to the 6 MeV statistical error on their average. The error in the overall energy scale has been estimated to be 24 MeV in a very recent report [31]. Here the 30 MeV conservative estimate used by the experiments until now has been assumed.

In the total width one can expect some common systematic error, such as that introduced by point to point variations in the normalization of the cross-section due to the uncertainty on the exact LEP energy setting at each point, or that introduced by the deconvolution of the initial state radiation. A conservative 10 MeV common error due to these possible effects has been assumed here. It has been quadratically subtracted from each quoted error and quadratically added to the resulting average. The invisible width is also affected by this 10 MeV error.

The main common error on the hadronic peak cross-section is that due to the theoretical uncertainty in the Bhabha cross-section at low angles. The error quoted by each individual experiment (0.7% by ALEPH and L3, 1% by DELPHI and OPAL) has been taken off from the corresponding measurement, and a 1% error has been added to the resulting average to obtain the number quoted in Table 3.

The hadronic and leptonic widths are also affected by the error in the Bhabha cross-section at low angles. Since the cross-section depends quadratically on the widths, this common error is taken as 1/2 of that on the cross-section. The partial widths into electrons and the average partial width into leptons are affected in addition by the error in the t-channel subtraction, which is quoted by each experiment. The contribution to the error on  $\Gamma_e$  and  $\Gamma_l$  has been taken into account before making the average. The common error assumed for the widths is 0.5 % from the normalization and an additional 0.5 % (0.2 %) for  $\Gamma_e$  ( $\Gamma_l$ ) coming from the t-channel subtraction.

The comparison of the individual measurements of the LEP experiments and their averages with the Standard Model predictions are given in figures 8 to 14. The  $\chi^2/d.o.f.$  of the different measurements with respect to their averages is also shown in the figures. The Standard Model prediction numbers refer to the limits of the interval of variation on each quantity. To compute this interval the Standard Model parameters were allowed to vary, the mass of the Z in the range (91.177-0.031) GeV to (91.177+0.031) GeV, the strong coupling constant  $\alpha_s$  between 0.10 and 0.14, the mass of the top between 80 GeV and 240 GeV and the mass of the Higgs between 40 GeV and 1000 GeV. The program GAMMAZ [35] was used to compute the Standard Model predictions.

The conclusion from this comparison is that all the averages of the model-independent parameters as measured at LEP and SLC differ by less than 1  $\sigma$  of their error from the Standard Model predictions, if the parameters of the Standard Model are allowed to vary in the range indicated. Figures 8 to 14 show graphically the results.

## 6 Constraining the Standard Model parameters.

### 6.1 The determination of the number of light neutrino species

One of the first and more fundamental measurements done by the SLC and LEP experiments has been the determination of the number of light neutrino families [10]-[14]. This number is inferred, within the framework of the Standard Model, from the measurement of the invisible width extracted from the line shapes.

Assuming that  $\Gamma_{inv}$  is entirely due to neutrinos and that the partial widths into the different kinds of neutrinos are equal,  $\Gamma_\nu$ , one has

$$\Gamma_{inv} = N_\nu \cdot \Gamma_\nu \quad (12)$$

where  $N_\nu$  is the number of neutrino families to which the Z couples. Assuming the Standard Model prediction for the partial width into a light neutrino,  $\Gamma_\nu = 167.3 \pm 1.6 MeV$ , the value  $N_\nu = 2.88 \pm 0.10$  results from the average LEP values of the invisible width.

$N_\nu$  can alternatively be obtained by combining the measurements of the invisible width and hadronic peak cross-section. From formulas 10 and 11 one obtains

$$N_\nu = \frac{\Gamma_l}{\Gamma_\nu} \left( \sqrt{\frac{12\pi R}{M_Z^2 \sigma_h^0}} - R - 3 \right) \quad (13)$$

Using the Standard Model predictions  $(\Gamma_l/\Gamma_\nu)_{SM} = 0.5010 \pm 0.0005$ ,  $R_{SM} = (\Gamma_h/\Gamma_l)_{SM} = 20.76 \pm 0.14$ , one obtains the value  $N_\nu = 2.94 \pm 0.09$ . The advantage of this second method is that one has to assume only the Standard Model prediction for the ratios  $\Gamma_l/\Gamma_\nu$  and  $\Gamma_h/\Gamma_l$  which depend little on the unknown top and Higgs masses.

If the average LEP result,  $R = 21.08 \pm 0.20$ , is used instead of the Standard Model prediction, the result is

$$N_\nu = 2.89 \pm 0.10 \quad (14)$$

In this case the only Standard Model assumption is  $\Gamma_l/\Gamma_\nu$ . The result would still be valid if unexpected states giving hadrons were present in Z decays. The dominant contribution to the error on  $N_\nu$  comes from the error on  $\sigma_h^0$ , which is in turn dominated, for each experiment, by the error on the luminosity (see section 6).

### 6.2 The determination of $\sin^2 \theta_W$

It was mentioned in section 3 above that most of the radiative corrections other than photon radiation from the initial state could be included in the s dependent

width of formula (7) and in the Z widths. One way of accomplishing this is by calculating the widths in the improved Born approximation where all the coupling constants become “running constants” [32], [3], [20]. The improved Born calculation includes all the large parts of the electroweak corrections. What is not included are small corrections coming from imaginary parts of self-energies, boxes and vertices. These additional corrections, together with other factorizable corrections, such as final state photon radiation and, in the case of the hadrons, gluon radiation, can also be incorporated in the width in the form of a small multiplicative factor [2]

$$E = (1 + \kappa)(1 + \Delta_{vertex})(1 + \delta_{QED})(1 + \delta_{QCD}) \quad (15)$$

$$\Gamma_f = E \frac{\alpha(M_Z^2) M_Z N_C}{48 \sin^2 \theta_W(M_Z^2) \cos^2 \theta_W(M_Z^2)} \left[ \left( 1 + \left( 1 - 4 \sin^2 \theta_W(M_Z^2) \right)^2 \right) \right] \quad (16)$$

where the mass of the fermion  $f$  has been neglected.

In this formula  $(1 + \kappa) = (0.2 \pm 0.3)10^{-2}$  [33] is included to accommodate some of the small additional electroweak corrections,  $\Delta_{vertex}$  comes from vertex corrections and in practice is only important for the  $b\bar{b}$  final state [34],  $\delta_{QED} = 3/4 \times \alpha/\pi$  comes from final state photon radiation, and  $\delta_{QCD} = \alpha_s/\pi + 1.405(\alpha_s/\pi)^2$  [4] comes from gluon radiation in the case of  $q\bar{q}$  final state.

The quantities  $\alpha(M_Z^2)$  and  $\sin^2 \theta_W(M_Z^2)$  are running parameters.  $\alpha(M_Z^2) = \alpha/(1 - \Delta\alpha)$  where  $\Delta\alpha$  at  $M_Z^2$  represents a 6% correction to  $\alpha$  at  $Q^2 = 0$ :  $\alpha(M_Z^2) = 1/128.7$  [3]. The running  $\sin^2 \theta_W(M_Z^2)$  is related to  $M_Z$  by the relation, valid in the improved Born approximation, [3]

$$\sin^2 \theta_W(M_Z^2) = \frac{1}{2} \left( 1 - \sqrt{1 - \frac{4\pi\alpha(M_Z^2)}{\sqrt{2}G_F\bar{\rho}M_Z^2}} \right) \quad (17)$$

where, in the Minimal Standard Model,  $\bar{\rho} \approx 1 + \Delta\rho$ . Most of the electroweak corrections, and therefore the dependence of the width on the unknown top and Higgs masses, are contained in  $\Delta\rho$  (see section 6.4).

The effective parameter  $\sin^2 \theta_W(M_Z^2)$  can then be obtained from the measurements of  $M_Z$  and the widths, in particular from the leptonic and total widths. ALEPH obtains  $\sin^2 \theta_W(M_Z^2) = 0.2291 \pm 0.0040$  [15] and DELPHI obtains  $\sin^2 \theta_W(M_Z^2) = 0.2309 \pm 0.0048$  [16]. In both cases the value comes from the measurement of  $M_Z$  and of the leptonic width. From the mass and the total width L3 obtains  $\sin^2 \theta_W(M_Z^2) = 0.230 \pm 0.004$  [17]. From formula (17) L3 also obtains  $\bar{\rho} = 1.005 \pm 0.012$ .

The measurement of the widths can be combined with other observables at LEP, in particular with the forward-backward charge asymmetry of leptons, to obtain more precise values of  $\sin^2 \theta_W(M_Z^2)$ . At the peak of the Z and assuming lepton universality the relation between the forward backward asymmetry and  $\sin^2 \theta_W(M_Z^2)$  is given by [6], [37]

$$A_{FB} \approx 3 \cdot \frac{g_{Vl}^2(M_Z^2)}{g_{Al}^2(M_Z^2)} \quad (18)$$

$$g_{Vl}(M_Z^2) = \frac{1}{2}\bar{\rho} (1 - 4 \sin^2 \theta_W(M_Z^2)) \quad (19)$$

$$g_{Al}(M_Z^2) = \frac{1}{2}\bar{\rho} \quad (20)$$

From a combined fit to the leptonic cross-section and forward-backward charge asymmetry OPAL obtains  $\bar{\rho} = 1.005 \pm 0.012$  and  $\sin^2 \theta_W(M_Z^2) = 0.2315 \pm 0.0028$  [18]. Other observables, such as the tau polarization asymmetry [37] and the forward-backward charge asymmetry for quarks can also be combined with the leptonic width and asymmetries. From the average of the  $\sin^2 \theta_W(M_Z^2)$  measured with all these observables ALEPH obtains  $\sin^2 \theta_W(M_Z^2) = 0.2283 \pm 0.0027$  [36].

Table 4 summarizes the values of  $\sin^2 \theta_W(M_Z^2)$  obtained by the different experiments. The average LEP result is

$$\sin^2 \theta_W(M_Z^2) = 0.2300 \pm 0.0020 \quad (21)$$

To calculate the error on this average a 0.6 % common systematic error (coming from the common systematic error on the width, see section 5), has been assumed.

It should be stressed that the value of the effective  $\sin^2 \theta_W(M_Z^2)$  extracted from the data incorporates radiative effects, including those due to the top and the Higgs, and is therefore valid regardless of the values of the masses of these particles.

### 6.3 The determination of $\alpha_s$

The ratio  $R = \Gamma_{had}/\Gamma_l$  can be written as

$$R = R^0(1 + \alpha_s(M_Z^2)/\pi + 1.405(\alpha_s(M_Z^2)/\pi)^2) \quad (22)$$

where the term in parenthesis is due to final state gluon radiation which, as pointed out in section 6.2 above, can be factorized from other radiative effects entering in the calculation of the hadronic width. (Higher order terms seem at present not yet known [9]). Since most of these effects cancel in the ratio of the hadronic to the leptonic widths, the quantity  $R^0$  is very well predicted in the Standard Model,  $R_{SM}^0 = 19.96 \pm 0.03$ . From the measured value of  $R$  and this Standard Model prediction of  $R^0$ , ALEPH [15] reports a value of  $\alpha_s = 0.13 \pm 0.06$ . The value obtained from the average LEP result,  $R = 21.08 \pm 0.20$ , and formula 22 above to second order, is

$$\alpha_s(M_Z^2) = 0.16 \pm 0.03 \quad (23)$$

The error in  $\alpha_s$ , obtained with this method is at present larger than that obtained from the analysis of hadronic events based on QCD, such as jet multiplicities and energy-energy correlations [8], [19]. However it is free from any hypothesis on non-perturbative phenomena, such as quark fragmentation.

## 6.4 The limits on the top mass

The measurements of the mass and widths of the Z at LEP, if interpreted within the framework of the Standard Model, do constraint the values of the top and Higgs masses. These values enter in the calculation of  $\Delta\rho$  in formula (17). In fact, this formula, which is also written as

$$\sin^2\theta_W(M_Z^2)\cos^2\theta_W(M_Z^2) = \frac{\pi\alpha}{\sqrt{2}G_F M_Z^2} \frac{1}{1 - \Delta\bar{r}} \quad (24)$$

can be viewed, for a given value of  $M_Z$ , as a relation between  $\sin^2\theta_W(M_Z^2)$  and the top and Higgs masses, since

$$\Delta\bar{r} = \Delta\alpha - \Delta\rho + \dots \quad (25)$$

$$\Delta\rho = \frac{\sqrt{2}G_F}{16\pi^2} \sum N_f^c \Delta m_f^2 + \dots \quad (26)$$

where  $\Delta\alpha$  is small and well known [3]. The sum in  $\Delta\rho$  extends to fermion doublets and  $\Delta m_f^2$  is the difference of the square of the masses of the particles in each doublet, and thus essentially  $m_{top}^2$ . The dots represent small terms entering the radiative correction calculations [3]. The dependence on the Higgs mass is contained on these terms and it is of the form  $\log M_H^2$ . From the measurement of  $M_Z$ , ALEPH obtains [15]

$$\sin^2\theta_W(M_Z^2) = 0.2316 \pm 0.0003 + 0.0024\left(1 - \left(\frac{m_t}{150\text{GeV}}\right)^2\right) + 0.0010 \log_{10} \frac{M_H}{200\text{GeV}} \quad (27)$$

The relation between  $\sin^2\theta_W(M_Z^2)$  and the top mass,  $m_t$ , imposed by the average  $M_Z$  value of the LEP experiments is shown in Fig. 15. To make this figure the Higgs mass was kept fixed at 200 GeV.

The expression for the width, formula(16), also establishes a relation between  $\sin^2\theta_W$  and the top and Higgs masses for a fixed value of  $\Gamma_{ff}$ , as it can be seen by combining (16) and (17) to eliminate  $M_Z$ . In particular, the measurements of the leptonic width (which is free from the corrections due to gluon radiation and therefore is not affected by the uncertainty in  $\alpha_s$ ) and the total width (which is measured with greater statistical precision), can both be used to relate  $\sin^2\theta_W(M_Z^2)$ ,  $m_t$  and  $M_H$ . These relations are also shown in Fig. 15 for the average LEP values of  $\Gamma_l$  and  $\Gamma_Z$ . To make the curves  $M_H$  was kept fixed at 200 GeV, and  $\alpha_s$  was fixed at 0.12.

The combination of the measurements of  $M_Z$ ,  $\Gamma_Z$  and  $\Gamma_l$  at LEP can then constrain  $m_t$ . From a combined fit to the hadronic and leptonic line shapes and

the leptonic forward-backward asymmetry, OPAL obtains

$$m_t = 154_{-94}^{+55} GeV \quad (28)$$

where an uncertainty in  $\alpha_s$  of  $\pm 0.02$  and a fixed Higgs mass of 100 GeV were assumed [13].

The LEP measurements can be combined with those of other observables to obtain more stringent limits. In particular the ratio of the masses  $M_W/M_Z$ , also provides a relation between  $\sin^2\theta_W(M_Z^2)$  and the top mass. In fact, the quantity

$$s_w^2 \equiv 1 - \frac{M_W^2}{M_Z^2} \quad (29)$$

is related to  $M_Z$  and the top and Higgs masses through [9]

$$s_w^2 c_w^2 = \frac{\pi\alpha}{\sqrt{2}G_F M_Z^2} \frac{1}{1 - \Delta r} \quad (30)$$

where  $c_w^2 \equiv 1 - s_w^2$  and

$$\Delta r = \Delta\alpha - \frac{c_w^2}{s_w^2} \Delta\rho + \dots \quad (31)$$

For fixed  $s_w^2$ , these equations, together with equations (17) and (23), do provide a relation between  $\sin^2\theta_W(M_Z^2)$  and the top and Higgs masses. The ratio of the masses has been measured directly by the UA2 experiment [38],  $M_W/M_Z = 0.8831 \pm 0.0055$ , and the W mass has been measured by the CDF experiment [39],  $M_W = 79.83 \pm 0.44$ , which can be combined with the LEP value of  $M_Z$  to obtain  $s_w^2$ . Neutrino experiments also measure  $s_w^2$ , as stressed in [40]. The combined result of CDHS [41] and CHARM [42] gives  $s_w^2 = 0.231 \pm 0.006$ . Combining all three results one obtains  $s_w^2 = 0.2295 \pm 0.0044$ . The relation between  $\sin^2\theta_W(M_Z^2)$  and  $m_t$  resulting from this value is also shown in Fig. 15.

An analysis, described in [43], of the data combining the measurements of  $M_Z$ ,  $\Gamma_Z$ ,  $\Gamma_h$  and  $\Gamma_l$  from L3 and  $s_w^2$  from the experiments mentioned above, has been presented to this conference giving

$$m_t = 141_{-42}^{+35} GeV \quad (32)$$

(The systematic error on  $M_Z$  coming from the error on the LEP energy scale was however not taken into account in the above errors).

Combining the measurements of  $M_Z$ ,  $\Gamma_l$  with the measurement of  $s_w^2$ , ALEPH obtains the following value for the top mass [15]

$$m_t = 120 \pm 40 \pm 3_{M_Z} \pm 1_{\alpha_s} \pm 20_{M_H} GeV \quad (33)$$

where the subscripts refer to the uncertainties coming from the quantities in the label.

From the fit to line shapes, leptonic forward-backward asymmetry and  $s_w^2 = 0.2254 \pm 0.0065$  (obtained from the measurements of UA2 and CDF), OPAL obtains [13]

$$m_t = 154_{-58}^{+39} GeV \quad (34)$$

where again the Higgs mass was kept fixed at 100 GeV. (The effect of varying the Higgs mass from 40 to 1000 GeV was also studied by OPAL, resulting on an increase on the upper error of about 20 GeV).

A fit similar to that of ALEPH, but using the average LEP values of  $M_Z$ ,  $\Gamma_Z$  and  $\Gamma_l$  instead, gives

$$m_t = 142_{-36}^{+31} \pm 20_{M_H} GeV \quad (35)$$

### Acknowledgements

I would like to thank the organizers of the Neutrino 90 Conference for the invitation to give this talk and the LEP Collaborations for making their data available. I greatly benefitted from conversations with A. Blondel, Ll. Garrido, M. Mannelli, M. Martínez, J. Sedgbeer, J. Steinberger and M. Winter in the course of preparing the talk and writing this contribution to the Proceedings.

## References

- [1] A thorough discussion of physics at the Z pole is contained in *Z Physics at LEP 1*, Edited by G. Altarelli, R. Kleiss and C. Verzegnassi CERN report 89-08 (1989) and references therein.
- [2] F.A. Berens. *et al.* "Z Line shape", Ref. 1, Vol. 1, pag. 89.
- [3] M. Consoli, W. Hollik and F. Jegerlehner, "Electroweak Radiative corrections for Z Physics", Ref. 1, Vol. 1, pag. 7.
- [4] G. Burgers, F. Jegerlehner, B. Kniehl and J. Kuhn, " $\Delta r$ , or the Relation between the Electroweak Couplings and the Weak Vector Boson Masses", Ref. 1 Vol. 1, pag. 55.
- [5] A. Borrelli *et al.*, Nucl. Phys. B333 (1990) 357.
- [6] U. Becker, These Proceedings.
- [7] M. J. Oreglia, These Proceedings.
- [8] J. Drees, These Proceedings.
- [9] G. Altarelli, These Proceedings.

- [10] ALEPH Collaboration, D. Decamp *et al.*, *Phys. Lett.*, B231 (1989) 519.  
 ALEPH Collaboration, D. Decamp *et al.*, *Phys. Lett.*, B234 (1990) 399.  
 ALEPH Collaboration, D. Decamp *et al.*, *Phys. Lett.*, B235 (1990) 339.
- [11] DELPHI Collaboration, P. Aarnio *et al.*, *Phys. Lett.*, B231 (1989) 539.  
 DELPHI Collaboration, P. Aarnio *et al.*, *Phys. Lett.*, B241 (1990) 425.  
 DELPHI Collaboration, P. Abreu *et al.*, *Phys. Lett.*, B241 (1990) 435.
- [12] L3 Collaboration, B. Adeva *et al.*, *Phys. Lett.*, B231 (1989) 509.  
 L3 Collaboration, B. Adeva *et al.*, *Phys. Lett.*, B236 (1990) 109.  
 L3 Collaboration, B. Adeva *et al.*, *Phys. Lett.*, B237 (1990) 136.  
 L3 Collaboration, B. Adeva *et al.*, *Phys. Lett.*, B238 (1990) 122.
- [13] OPAL Collaboration, M.Z. Akrawy *et al.*, *Phys. Lett.*, B231 (1989) 530.  
 OPAL Collaboration, M.Z. Akrawy *et al.*, *Phys. Lett.*, B235 (1990) 379.  
 OPAL Collaboration, M.Z. Akrawy *et al.*, *Phys. Lett.*, B240 (1990) 497.  
 OPAL Collaboration, M.Z. Akrawy *et al.*, Cern preprint CERN-EP/90-81.
- [14] MarkII Collaboration, G.S. Abrams *et al.*, *Phys. Rev. Lett.*, 63 (1989) 724.  
 MarkII Collaboration, G.S. Abrams *et al.*, *Phys. Rev. Lett.*, 63 (1989) 2173.
- [15] ALEPH Collaboration, D. Decamp *et al.*, CERN-PPE/90-104. Submitted to *Zeitschrift für Physik C*.  
 Talk by J.R. Hansen at 25th International Conference on High Energy Physics, Singapore, August 1990.
- [16] DELPHI Collaboration, P. Abreu *et al.*, Contributed paper to Singapore Conference and forthcoming CERN/PPE preprint.  
 Talk by U. Amaldi at 25th International Conference on High Energy Physics, Singapore, August 1990.
- [17] L3 Collaboration, B. Adeva *et al.*, L3 Preprints 8, 9 and 17. Submitted to *Phys. Lett.*.  
 Talk by S. J. Ting at 25th International Conference on High Energy Physics, Singapore, August 1990.
- [18] OPAL Collaboration Internal Physics Note 90-16, July 1990.  
 Talk by T. Mori at 25th International Conference on High Energy Physics, Singapore, August 1990.
- [19] F. Dydak. Results from LEP and SLC (Summary talk). in the "25th International Conference on High Energy Physics". Singapore. August 1990.
- [20] G. Altarelli in "Theory of precision electroweak experiments" in Proceedings of the XIV International Symposium on Leptons and Photon Interactions, pag. 286. Edited by M. Riordan.



- [21] See for example F.A. Berends, G. Burgers and W.L. van Neerven, Nucl.Phys. B297 (1988) 429 and Nucl.Phys. B304 (1988) 921. Also Ref. [2].
- [22] M. Martinez et al. Model Independent Fitting to the  $Z^0$  Line Shape. June 1990. CERN-PPE/90-109. Submitted to *Zeitschrift für Physik C*.
- [23] M. Greco. *Phys. Lett.*, B177 (1986) 97. See also M. Caffo *et al.*, Ref. 1, Vol. 1, pag. 171.
- [24] F. Aversa *et al.*, INFN-Frascati preprint LNF-90/049 (1990).
- [25] ALIBABA program by W.J.P. Beenakker, F.A. Berens and S.C. van der Marck (Institut-Lorentz, Leiden).
- [26] The ZFITTER/ZBIZON program package of D. Bardin *et al.*, DELPHI 89-71 PHYS 52 (1989). D. Bardin *et al.*, *Zeit. Phys. C*44 (1989) 493, and D. Bardin *et al.*, *Comp. Phys. Comm.* 59 (1990)303.
- [27] R. N. Cahn, *Phys. Rev. D*36 (1987) 2666.
- [28] D. Bardin *et al.*, in Ref. 1 and D. Bardin *et al.*, Berlin-Zeuthen preprint PHE-89-19 (1989).
- [29] Program ZFITTER, D.Yu. Bardin *et al.*, Berlin-Zeuthen preprint PHE 89-19, 1989.
- [30] L. Rolandi, talk given at XXVth Rencontres de Moriond, CERN report CERN-EP/90-64.
- [31] R. Bailey *et al.*, CERN report SL/90-95, August 1990.
- [32] D.C. Kennedy and B. W. Lynn, *Nucl. Phys.* B322 (1989) 1.
- [33]  $\kappa$  was calculated in ref. [15] using the program EXPOSTAR of D.C. Kennedy, B.W. Lynn, C.J.-C. Im and R.G. Stuart, *Nucl. Phys.* B321 (1989) 83.
- [34] J. H. Kuhn and P.M. Zerwas, "Heavy Flavors", Ref. 1 Vol. 1, pag. 269.
- [35] The GAMMAZ program was written by G. Burgers and W. Hollik.
- [36] ALEPH Collaboration: talk by J.C. Brient at 25th International Conference on High Energy Physics, Singapore, August 1990.
- [37] M. Böhm and W. Hollik. "Forward-Backward Asymmetries", Ref. 1, Vol. 1, pag. 203.
- [38] UA2 Collaboration, J. Alitti *et al.*, *Phys. Lett.* B241 (1990) 150.
- [39] CDF Collaboration, P. Shalbach, Proceedings of the APS conference, Washington DC, April 90.

- [40] A. Blondel, CERN preprint EP-89-84 (1989)
- [41] CDHS Collaboration H. Abramowicz et al., *Phys. Rev. Lett.* 57 (1986)298, and A. Blondel et al., *Z. Phys.* C45 (1990) 361.
- [42] CHARM Collaboration, J.V. Allaby et al., *Phys. Lett* B177 (1986)446, and *Z. Phys.* C36 (1987)611.
- [43] S. N. Ganguli and A. Gurtu, Tata Inst. Preprint TIFR-EHEP 90/1.

	ALEPH	DELPHI	L3	OPAL
No. of events	85000	68000	62000	112000
Syst. error	0.4%	1.1%	0.7%	0.8%
Luminosity syst. error	1.3%	1.7%	1.3%	1.6%

Table 1: Summary of the events samples used by the four LEP experiments to extract the hadronic line shapes.

	ALEPH	DELPHI	L3	OPAL
<b>Electrons</b>				
Angular range	$-0.9 < \cos \theta < 0.7$	$ \cos \theta  < 0.73$	$ \cos \theta  < 0.74$	$ \cos \theta  < 0.7$
No. of events	3548	1389	2642	3263
Syst. error	1.0%	1.3%	0.7%	1.0%
<b>Muons</b>				
Angular range	$ \cos \theta  < 0.90$	$ \cos \theta  < 0.73$	$ \cos \theta  < 0.8$	$ \cos \theta  < 0.95$
No. of events	3054	1618	1244	4642
Syst. error	0.9%	1.9%	1.5%	1.3%
<b>Taus</b>				
Angular range	$ \cos \theta  < 0.90$	$ \cos \theta  < 0.73$	$ \cos \theta  < 0.7$	$ \cos \theta  < 0.90$
No. of events	2971	1016	1169	3412
Syst. error	1.0%	2.7%	3.0%	2.0%
<b>Inclusive</b>				
Angular range	$-0.9 < \cos \theta < 0.7$	$ \cos \theta  < 0.64$		
No. of events	9455	3187		
Syst. error	0.6%	1.3%		

Table 2: Summary of the events samples used by the four LEP experiments to extract the leptonic line shapes.

	ALEPH	DELPHI	L3	OPAL	Average LEP
$M_Z$ $GeV/c^2$	$91.186 \pm 0.013_{stat}$	$91.188 \pm 0.013_{stat}$	$91.161 \pm 0.013_{stat}$	$91.174 \pm 0.011_{stat}$	$91.177 \pm 0.031$
$\Gamma_Z$ MeV	$2506 \pm 26$	$2476 \pm 28$	$2492 \pm 025$	$2505 \pm 20$	$2497 \pm 15$
$\Gamma_l$ MeV	$84.2 \pm 1.1$	$83.7 \pm 1.5$	$84.0 \pm 1.2$	$83.6 \pm 1.0$	$83.9 \pm 0.7$
$\Gamma_{had}$ MeV	$1764. \pm 23.$	$1756. \pm 30.$	$1748. \pm 35.$	$1778. \pm 26.$	$1764. \pm 16.$
$\Gamma_{inv}$ MeV	$489. \pm 22.$	$469. \pm 29.$	$494. \pm 32.$	$476. \pm 25.$	$482. \pm 16.$
$\Gamma_{had}/\Gamma_l$	$20.95 \pm 0.31$	$21.00 \pm 0.48$	$21.02 \pm 0.62$	$21.26 \pm 0.32$	$21.08 \pm 0.20$
$\sigma_{had}^0$ nb	$41.78 \pm 0.63$	$42.38 \pm 1.02$	$41.38 \pm 0.71$	$41.88 \pm 0.74$	$41.78 \pm 0.53$
$\Gamma_e$ MeV	$84.9 \pm 1.4$	$82.0 \pm 1.9$	$84.3 \pm 1.6$	$82.7 \pm 1.3$	$83.6 \pm 0.9$
$\Gamma_\mu$ MeV	$80.7 \pm 2.2$	$87.2 \pm 3.5$	$82.3 \pm 2.9$	$85.9 \pm 2.0$	$83.8 \pm 1.2$
$\Gamma_\tau$ MeV	$81.8 \pm 2.2$	$86.0 \pm 4.1$	$83.5 \pm 3.7$	$83.9 \pm 2.3$	$83.3 \pm 1.4$

Table 3: The electroweak parameters obtained by the four LEP experiments from fits of the line shapes. The errors on  $M_Z$  for the four experiments are statistical only. The errors on all the other parameters result from adding in quadrature statistical and systematic errors. The error on the averages have been obtained taking into account the common systematic errors, as explained in the text.

	$\sin^2\theta_W(M_Z^2)$	Observables
ALEPH	$0.2283 \pm 0.0027$	$M_Z, \Gamma_l, \tau$ polarization $l\bar{l}$ and $q\bar{q}$ forward-backward asymmetries
DELPHI	$0.2309 \pm 0.0048$	$M_Z, \Gamma_l$
L3	$0.230 \pm 0.004$	$M_Z, \Gamma_Z$
OPAL	$0.2315 \pm 0.0028$	$M_Z, \Gamma_l$ , $l\bar{l}$ forward-backward asymmetry
LEP	$0.2300 \pm 0.0020$	Average of the LEP experiments with common systematic error

Table 4:  $\sin^2\theta_W(M_Z^2)$  obtained by the four LEP experiments from different observables. The error on the average includes a common systematic error to all experiments, which is estimated to be 0.6% of the value of  $\sin^2\theta_W(M_Z^2)$ .

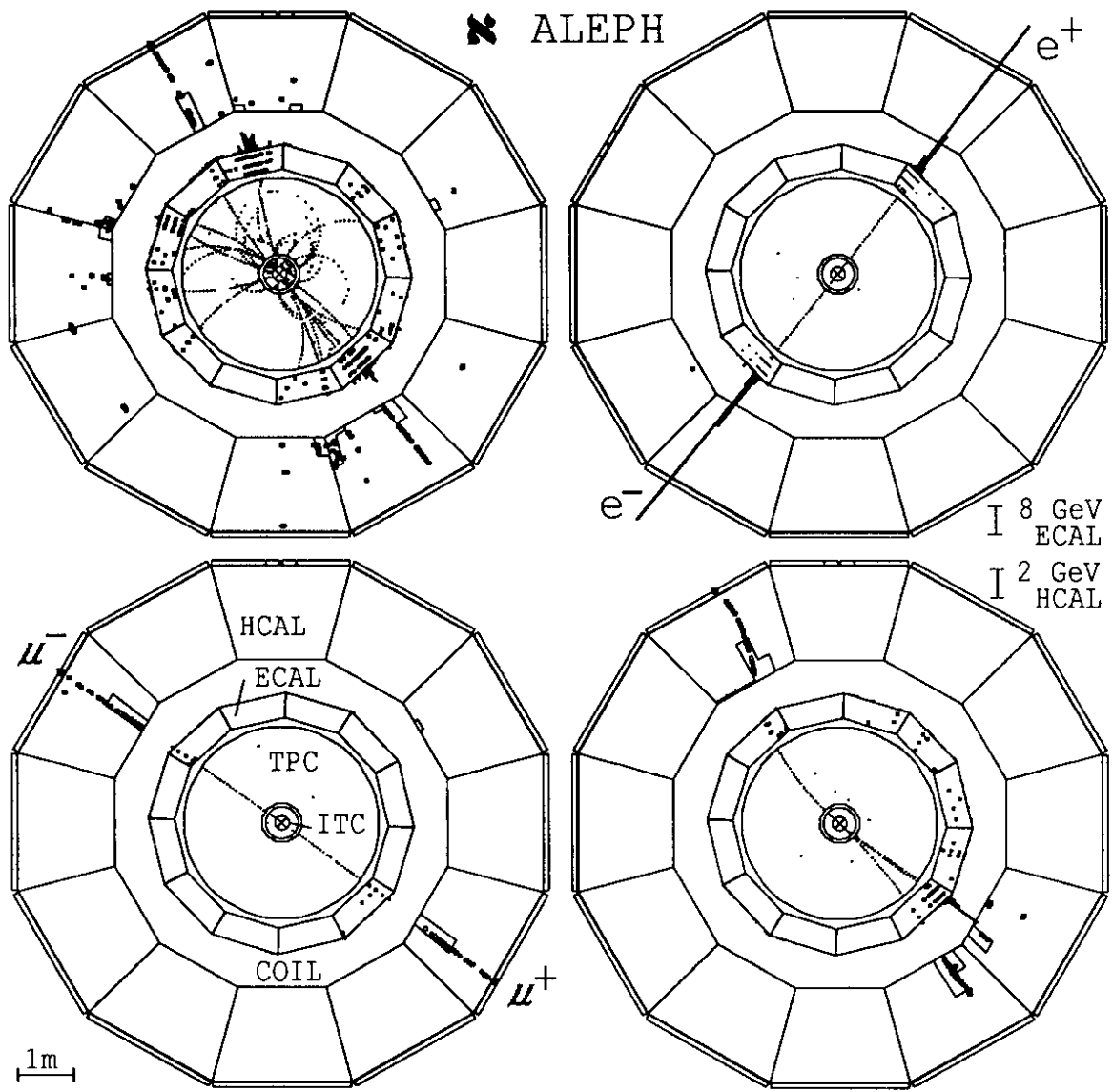


Figure 1: Display of Z decays into hadrons, and  $e^+e^-$ ,  $\mu^+\mu^-$  and  $\tau^+\tau^-$  pairs seen in the ALEPH detector.

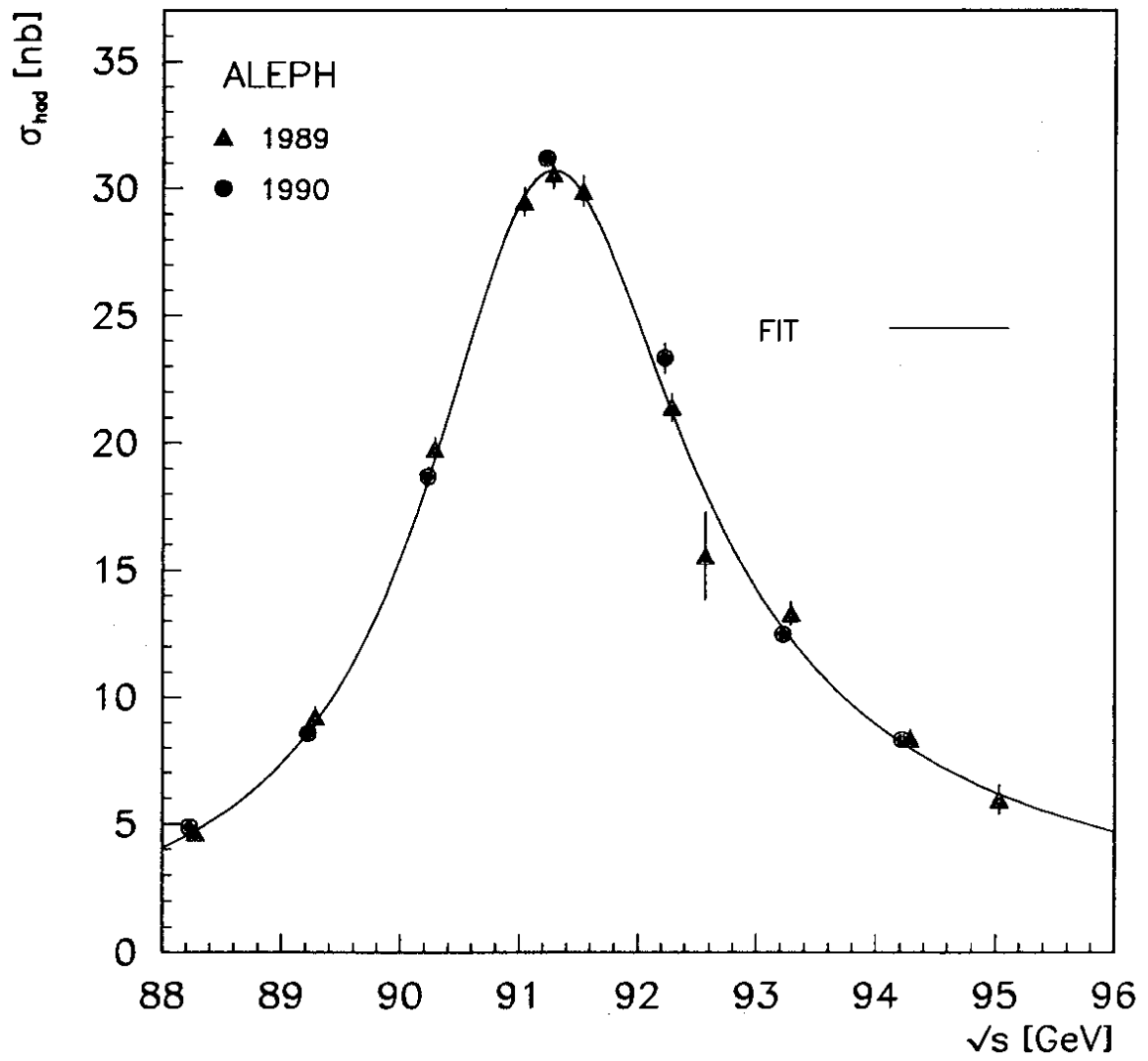


Figure 2: The ALEPH hadronic line shape



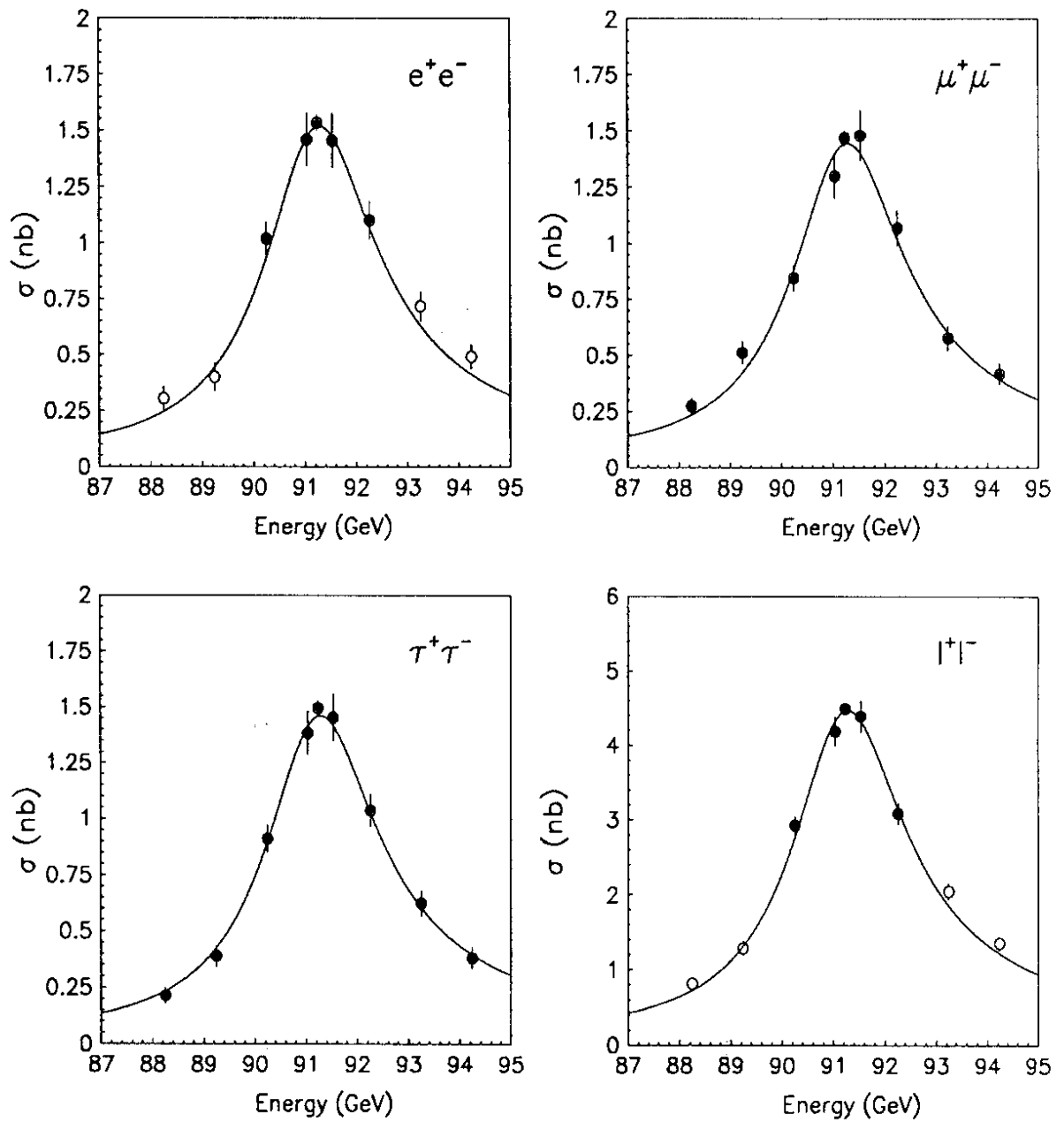


Figure 3: The ALEPH leptonic line shapes

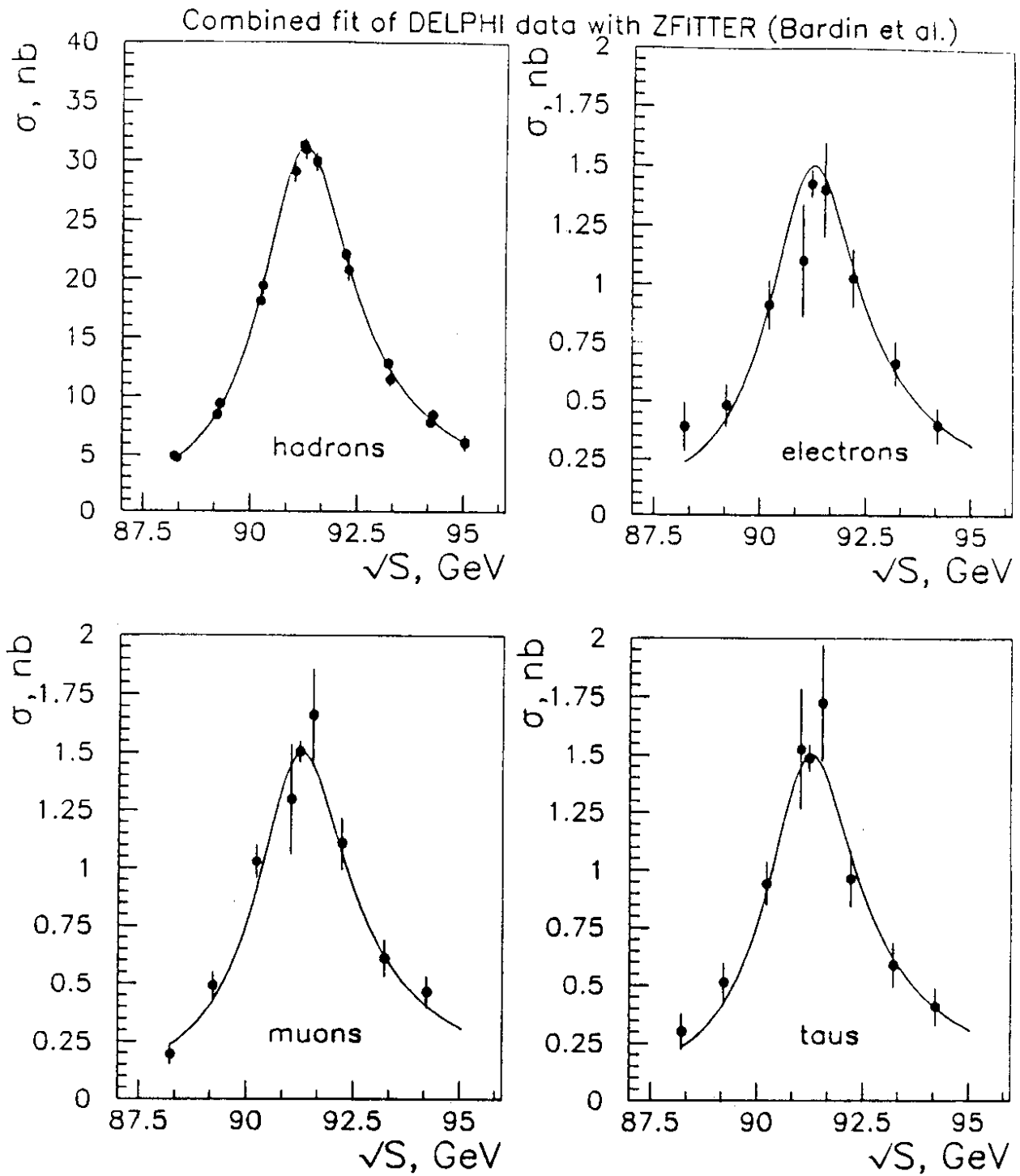


Figure 4: The DELPHI hadronic and leptonic line shapes

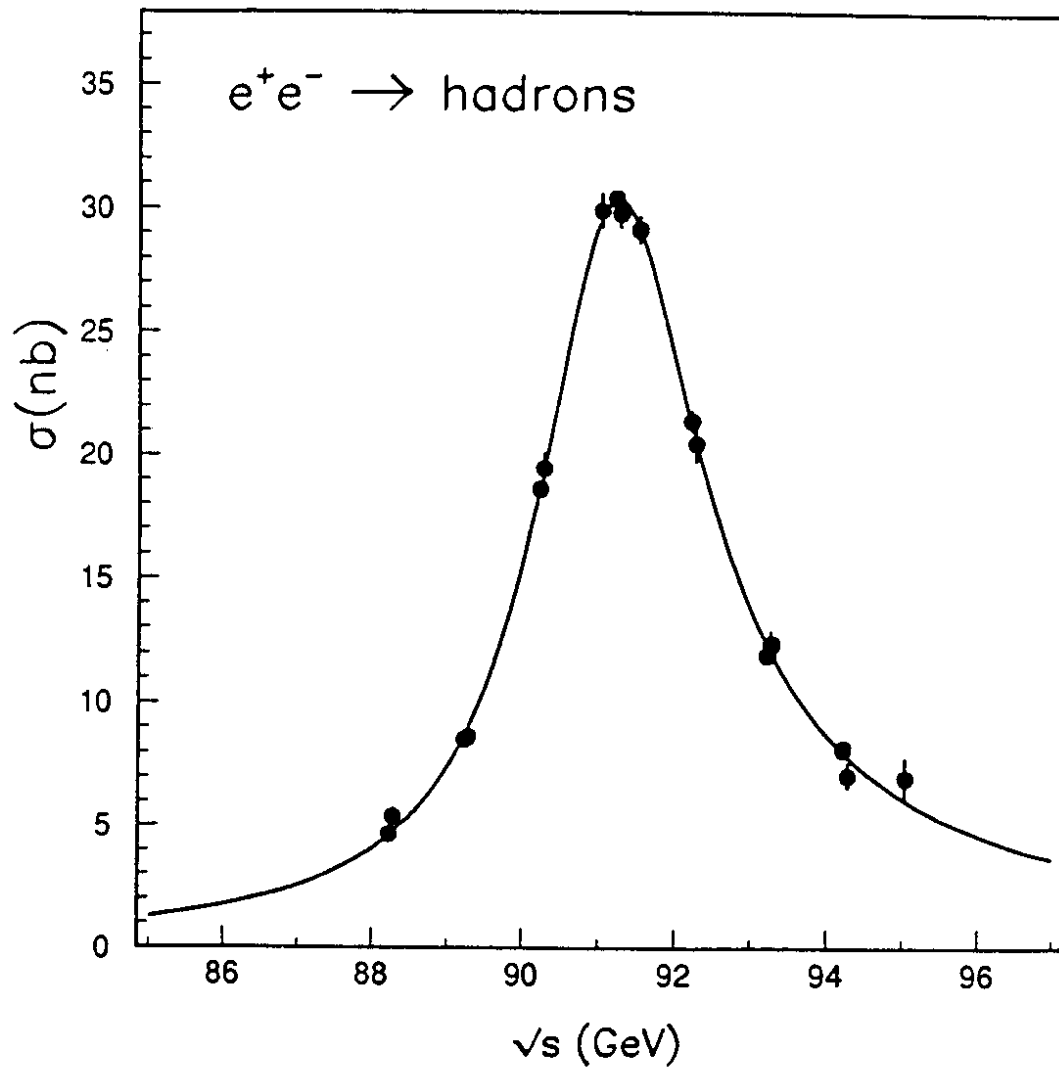
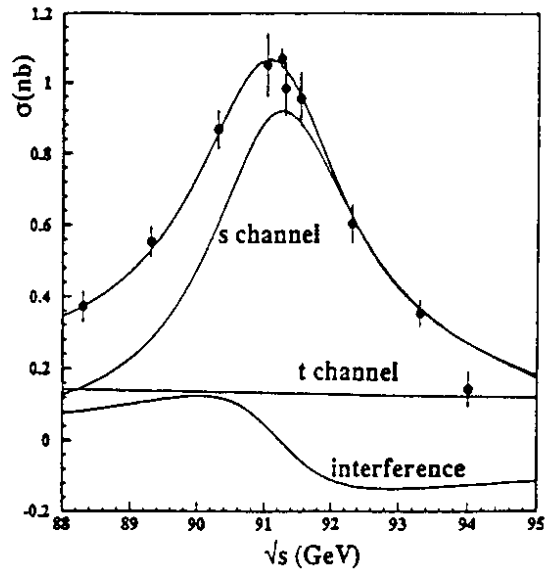
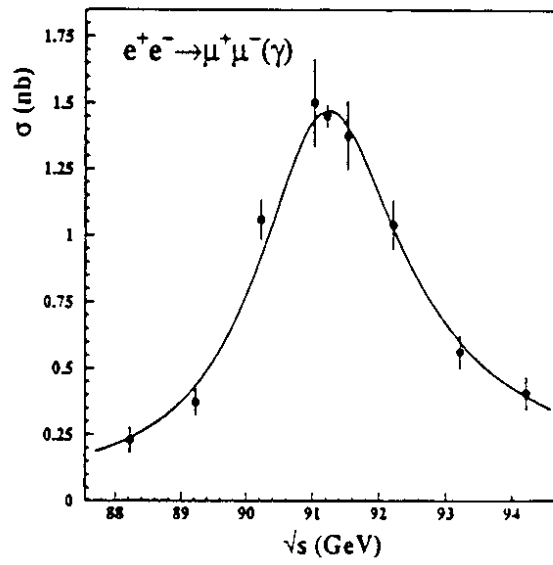


Figure 5: The L3 hadronic line shape

(a)



(b)



(c)

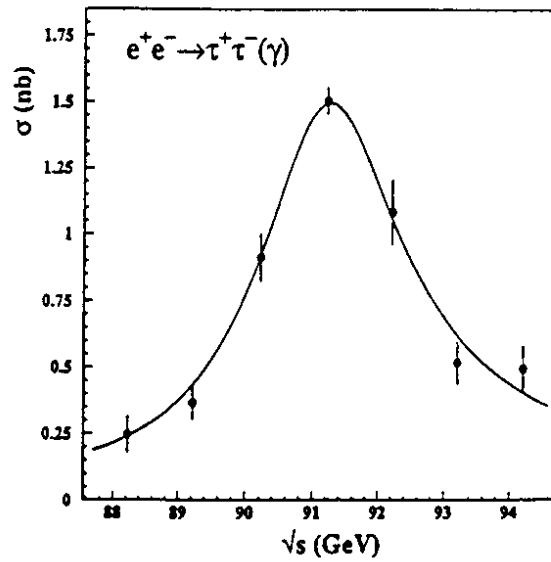


Figure 6: The L3 leptonic line shapes

# OPAL

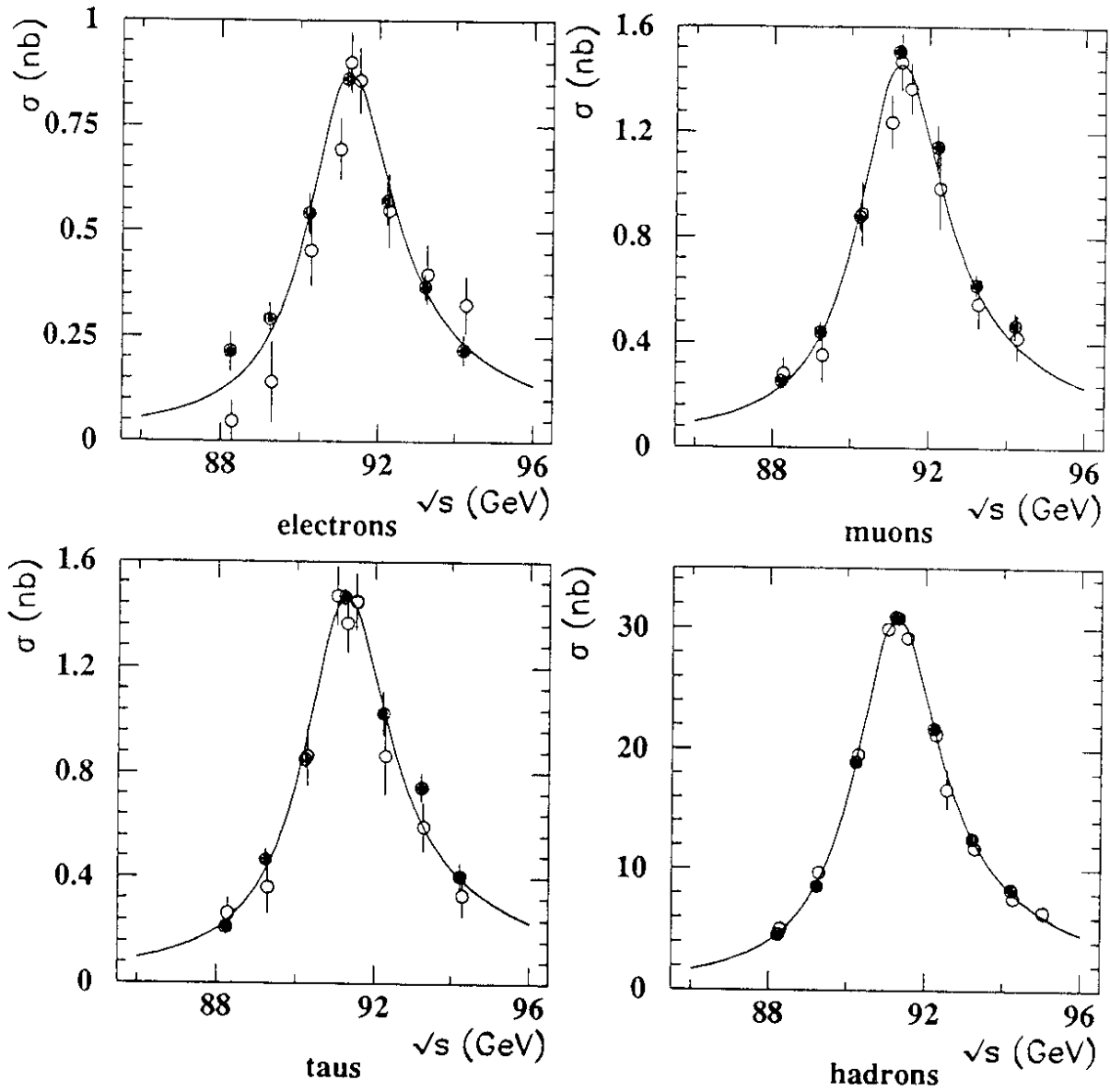


Figure 7: The OPAL hadronic and leptonic line shapes

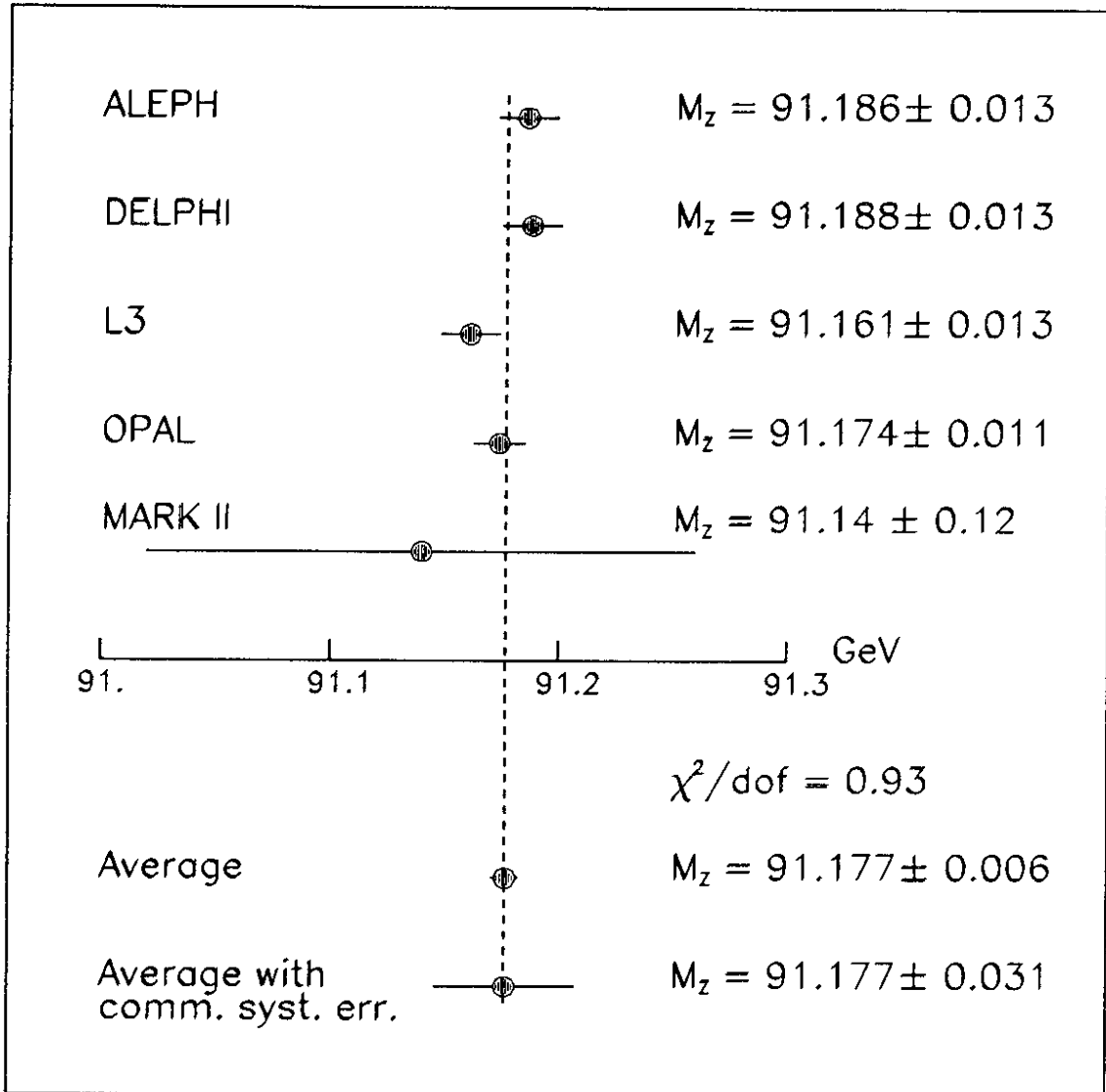


Figure 8: The mass of the Z from LEP and SLC.

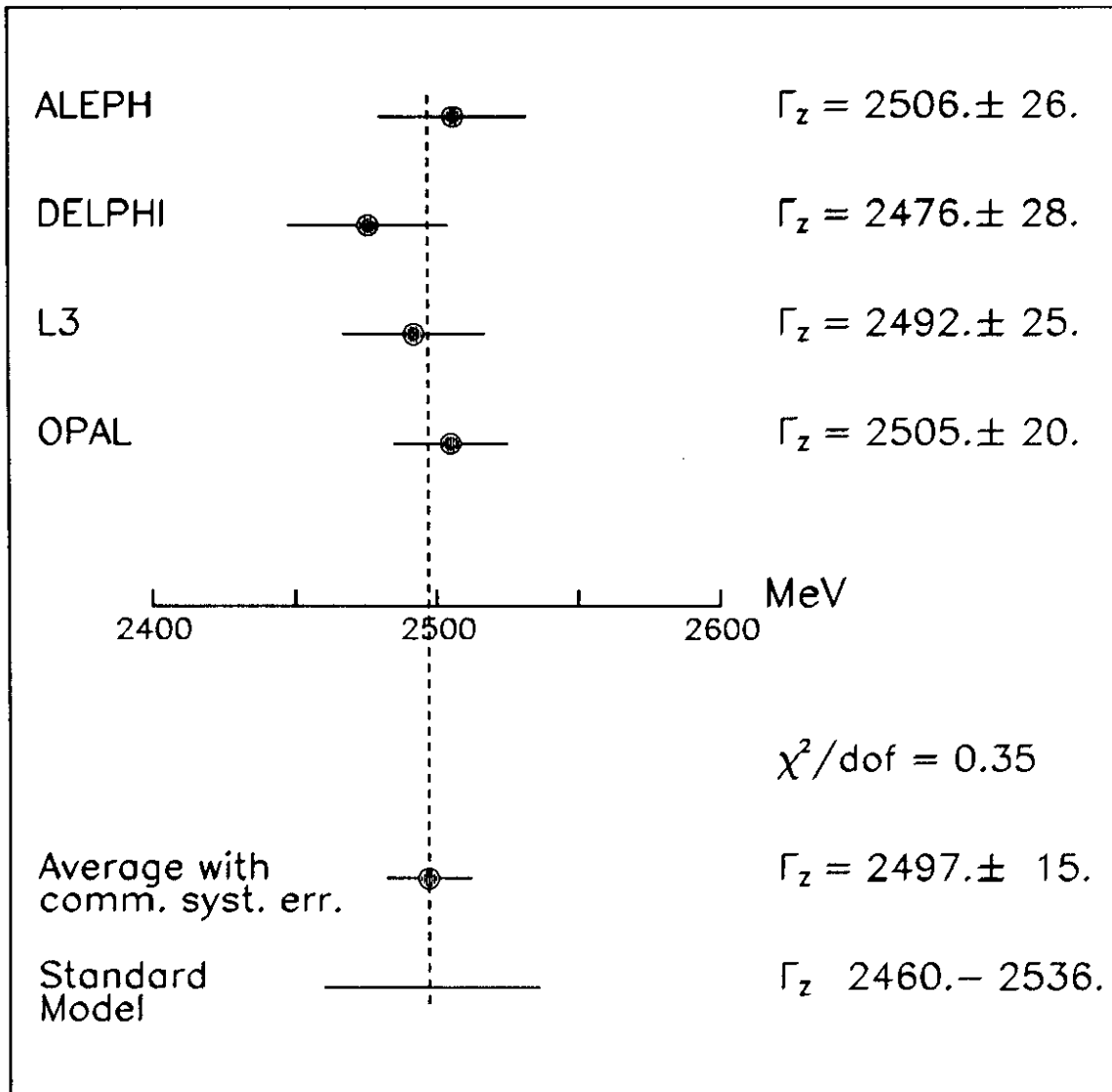


Figure 9: The total width of the Z from the LEP experiments.

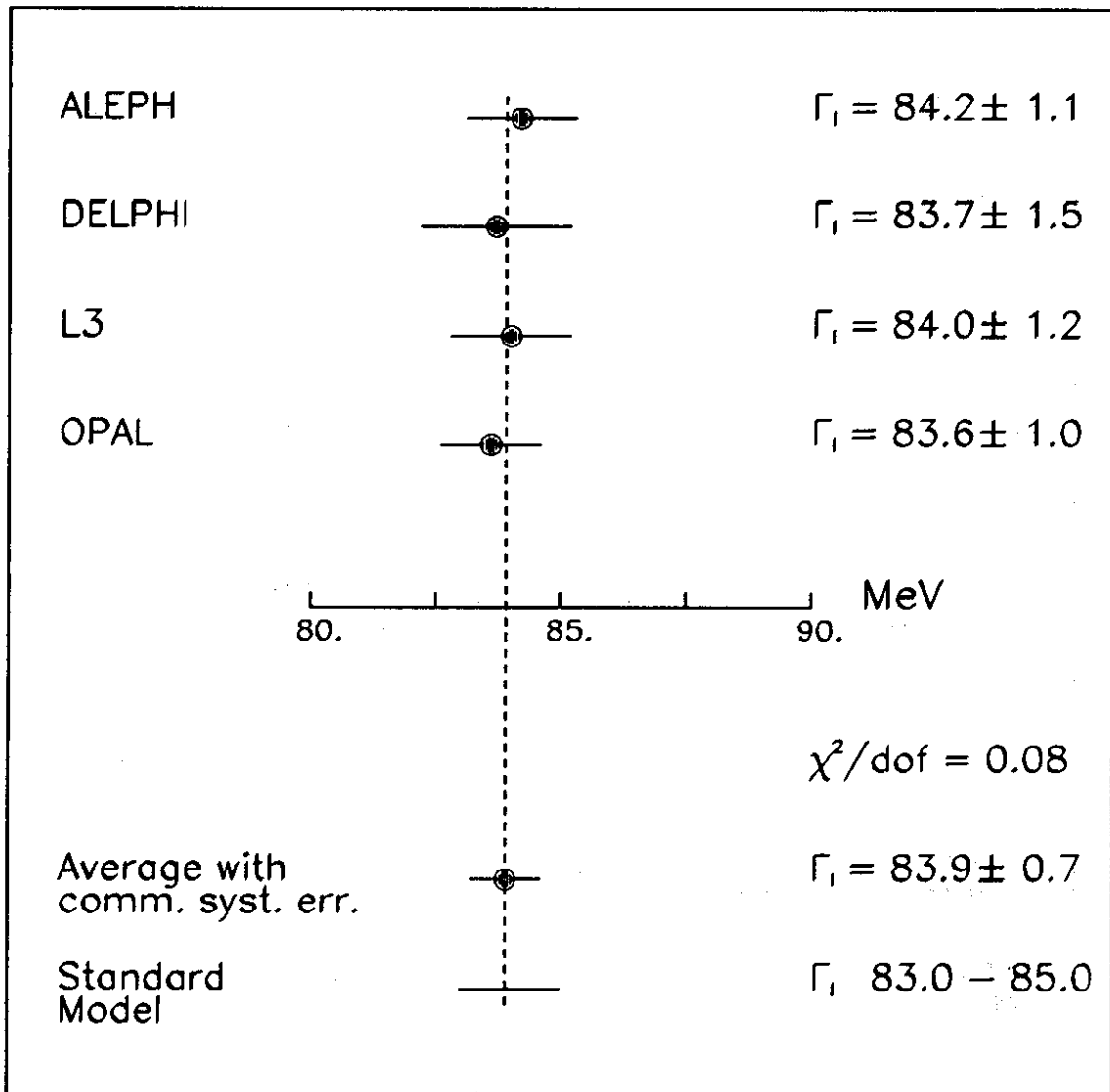


Figure 10: The leptonic width of the Z from the LEP experiments.



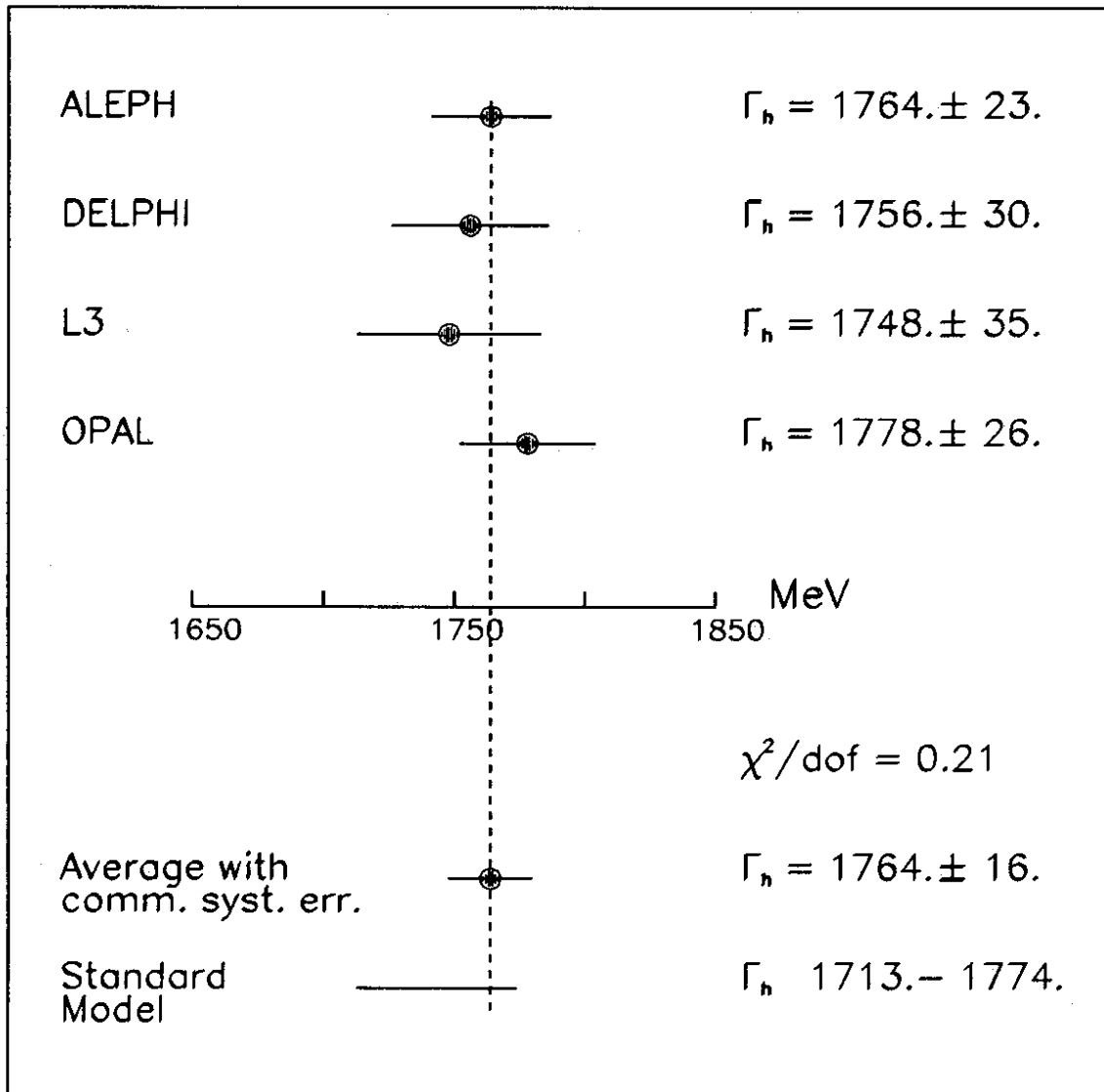


Figure 11: The hadronic width of the Z from the LEP experiments.

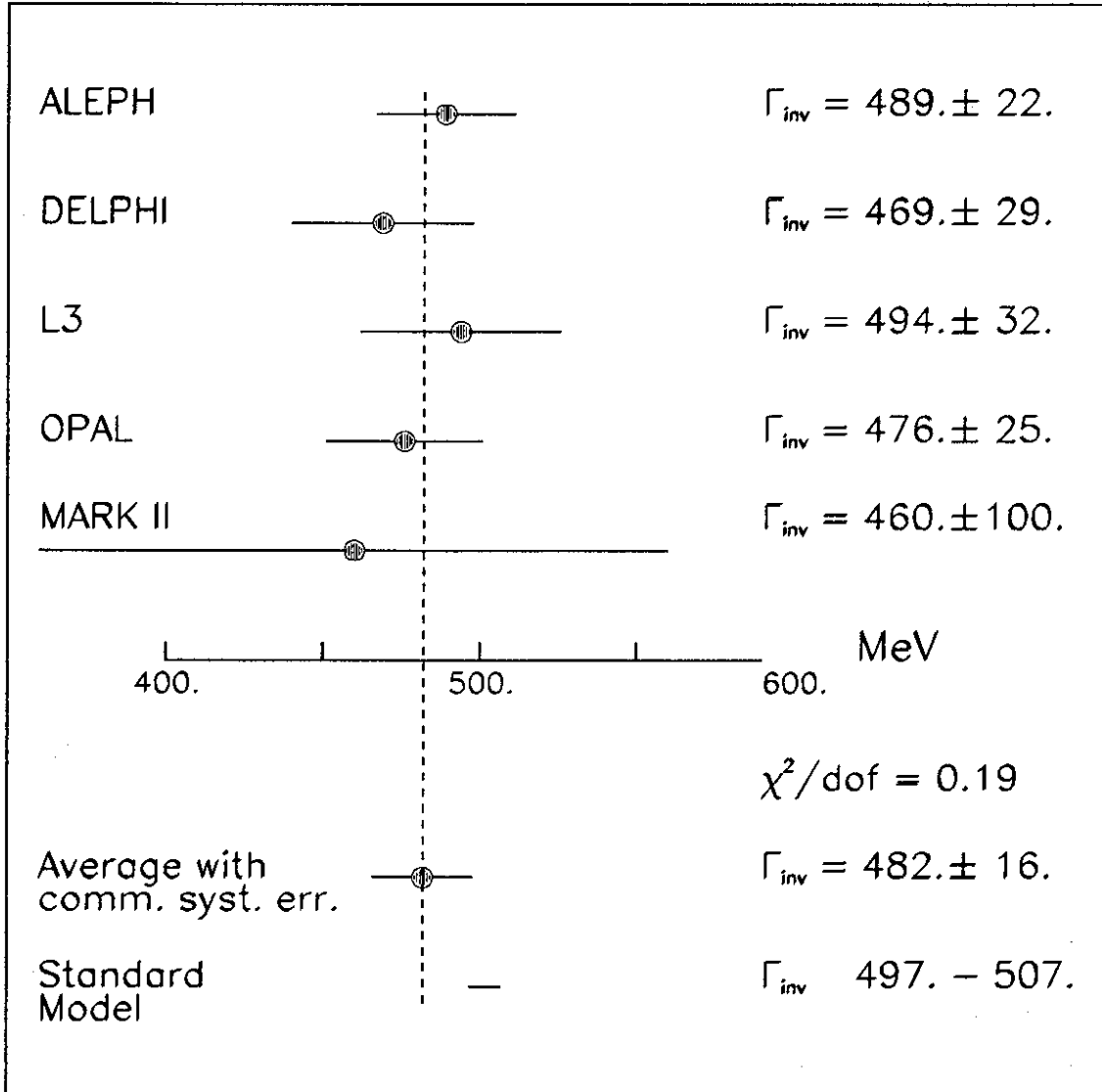


Figure 12: The invisible width of the Z from LEP and SLC.

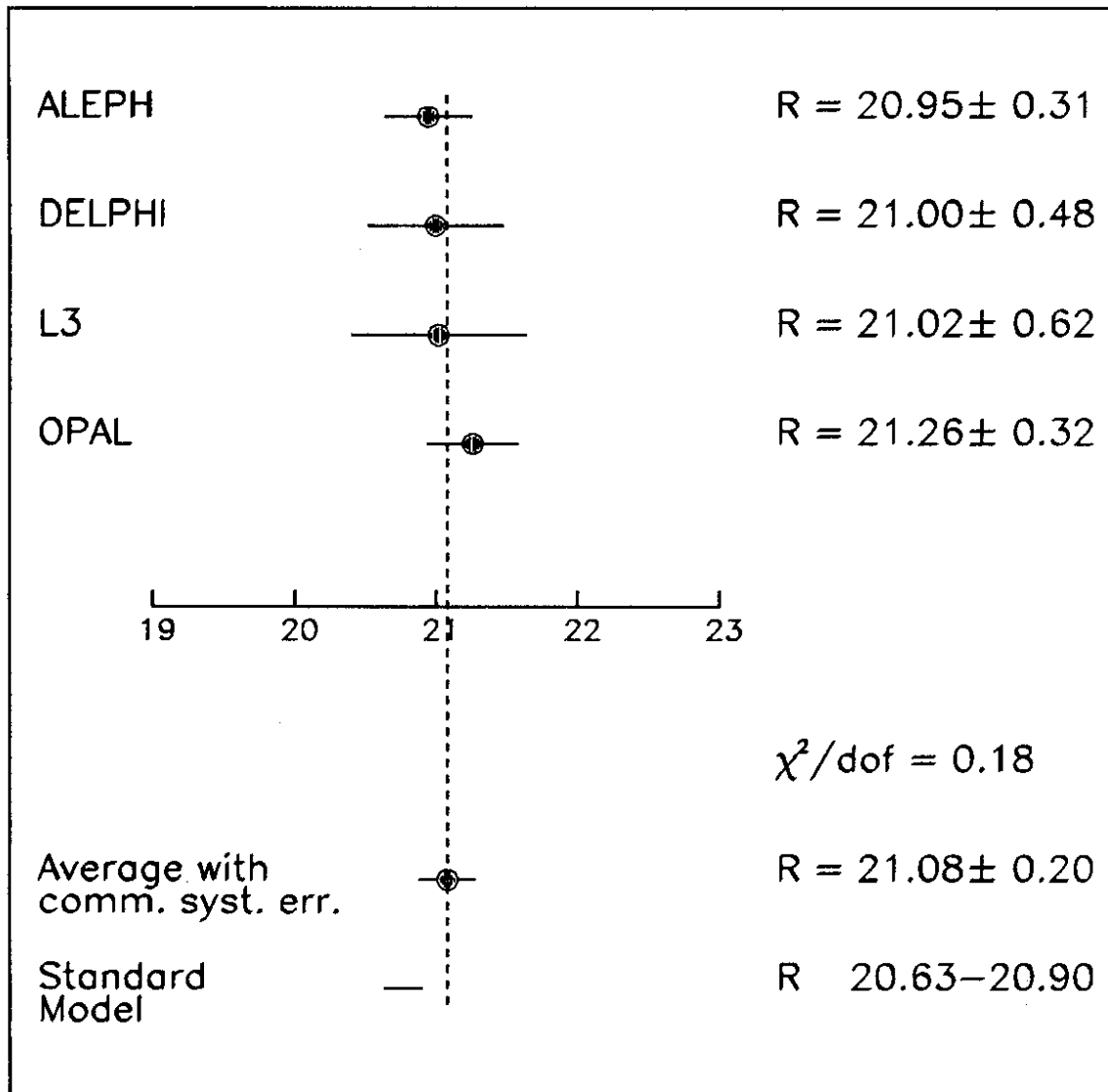


Figure 13: The ratio of the hadronic to the leptonic width.

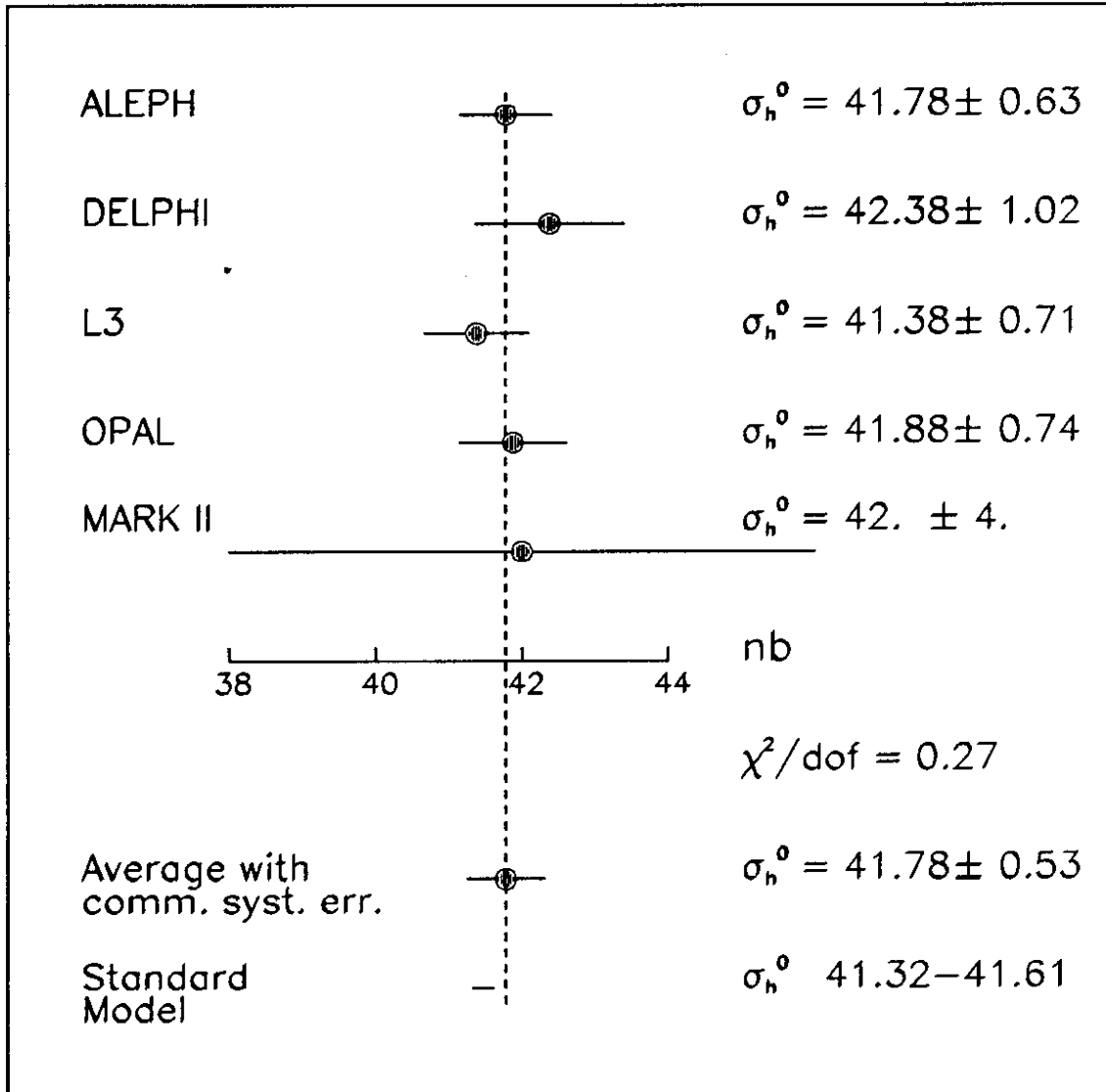


Figure 14: The hadronic peak cross-section.

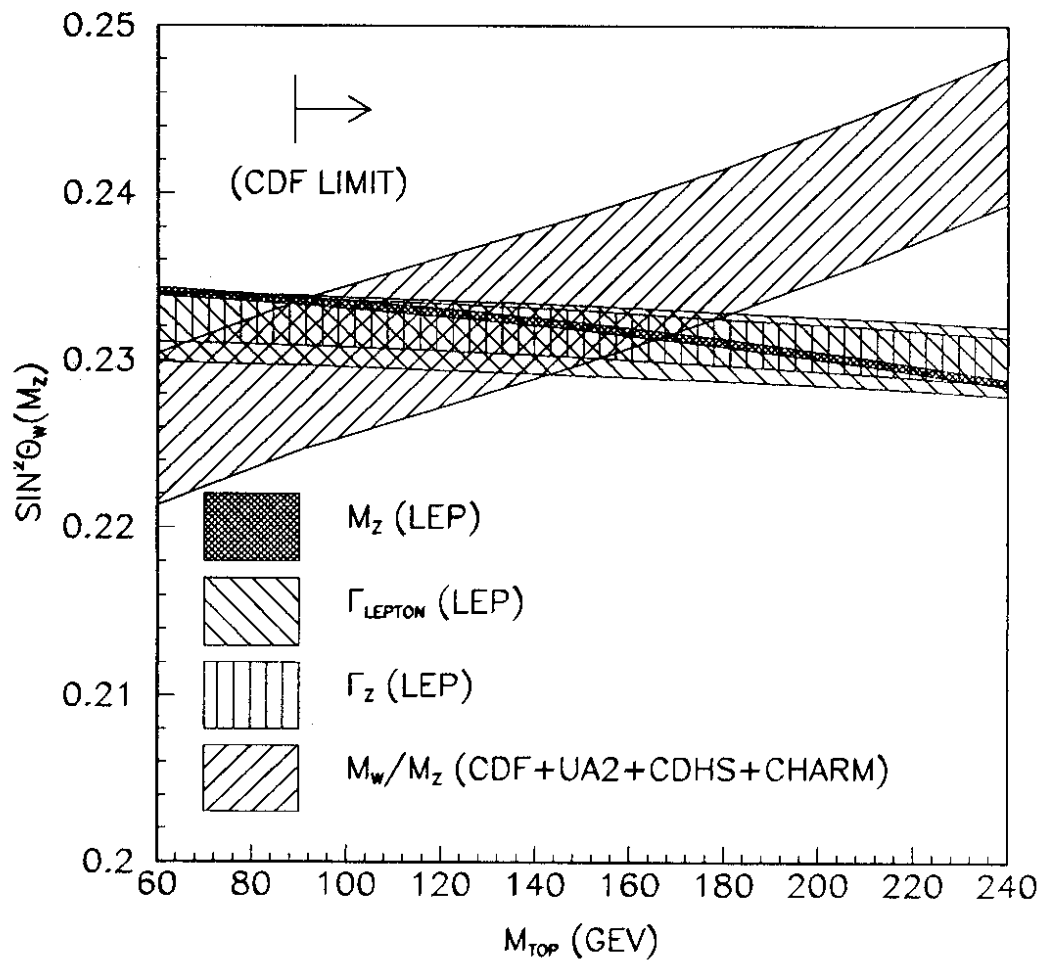


Figure 15: Constraints on  $\sin^2 \theta_W(M_Z^2)$  and the top mass from several observables.